Association of Functional Loss With the Biomechanical Response of the Optic Nerve Head to Acute Transient Intraocular Pressure Elevations

Tin A. Tun, MD; Eray Atalay, MD; Mani Baskaran, DNB, PhD; Monisha E. Nongpiur, MD, PhD; Hla M. Htoon, PhD; David Goh, FRCOphth; Ching-Yu Cheng, MD, PhD; Shamira A. Perera, FRCOphth; Tin Aung, FRCS(Ed), PhD; Nicholas G. Strouthidis, FRCS(Ed), PhD; Michaël J. A. Girard, PhD

➕ Supplemental content

IMPORTANCE The acute biomechanical response of the optic nerve head (ONH) to intraocular pressure (IOP) elevations may serve as a biomarker for the development and progression of glaucoma.

OBJECTIVE To evaluate the association between visual field loss and the biomechanical response of the ONH to acute transient IOP elevations.

DESIGN, SETTING, AND PARTICIPANTS In this observational study, 91 Chinese patients (23 with primary open-angle glaucoma [POAG], 45 with primary angle-closure glaucoma, and 23 without glaucoma) were recruited from September 3, 2014, through February 2, 2017. Optical coherence tomography scans of the ONH were acquired at baseline and at 2 sequential IOP elevations (0.64 N and then 0.90 N, by applying forces to the anterior sclera using an ophthalmodynamometer). In each optical coherence tomography volume, lamina cribrosa depth (LCD) and minimum rim width (MRW) were calculated. The mean deviation (MD) and the visual field index (VFI), as assessed by automated perimetry, were correlated with IOP-induced changes of LCD and MRW globally and sectorially.

MAIN OUTCOMES AND MEASURES The LCD, MRW, MD, and VFI.

RESULTS Among the 91 patients, 39 (42.9%) were women; the mean (SD) age was 65.48 (7.23) years. In POAG eyes, a greater change in LCD (anterior displacement) was associated with worse MD and VFI ($R = -0.64$; 95% CI, -0.97 to -0.31; $P = .001$; and $R = -0.57$; 95% CI, -0.94 to -0.19; $P = .005$, respectively) at the first IOP elevation, and a greater reduction in MRW was also associated with worse MD and VFI (first IOP elevation: $R = -0.48$; 95% CI, -0.86 to -0.09; $P = .02$; and $R = -0.57$; 95% CI, -0.94 to -0.20; $P = .004$, respectively; second IOP elevation: $R = -0.56$; 95% CI, -0.98 to -0.13; $P = .01$; and $R = -0.60$; 95% CI, -1.03 to -0.17; $P = .008$, respectively), after adjusting for age, sex, and baseline IOP. A correlation was found between the reduction in MRW in the inferior-temporal sector and the corresponding visual field cluster in POAG eyes at the second elevation ($\rho = -0.55$; 95% CI, -0.78 to -0.18; $P = .006$).

CONCLUSIONS AND RELEVANCE The biomechanical response of the ONH to acute IOP elevations was associated with established visual field loss in POAG eyes, but not in primary angle-closure glaucoma eyes. This suggests that ONH biomechanics may be related to glaucoma severity in POAG and that the 2 glaucoma subgroups exhibit inherently different biomechanical properties.

Author Affiliations: Author affiliations are listed at the end of this article.

Corresponding Author: Michaël J. A. Girard, PhD, Ophthalmic Engineering and Innovation Laboratory, Department of Biomedical Engineering, National University of Singapore, 4 Engineering Dr 3, E4-04-08, 117583, Singapore (mgirard @nus.edu.sg).

The lamina cribrosa (LC) is thought to be the main site of damage to retinal ganglion cell axons, which occurs at the onset and during the course of glaucoma.[1] Glaucomatous damage is typically characterized by functional loss (the pattern of visual field [VF] defects) and structural changes such as distinct cupping of the optic nerve head (ONH) and thinning of the retinal nerve fiber layer (RNFL).[2]

Spectral-domain optical coherence tomography (SD-OCT) allows the deep structures of the eye, particularly the RNFL, the neuroretinal rim (NRR), and the LC, to be assessed in vivo through volumetric imaging with interpolated B-scans that closely match histologic sections.[3] Thus, small-scale structural changes of the LC[4] (a sign of cupping) and of the minimum rim width[5,6] (MRW), a sign of RNFL thinning at the NRR, can be objectively measured.

Structure-function relationships in glaucomatous eyes have been reported by various studies using SD-OCT.[7-10] Such relationships may help us understand the pathogenesis and monitor glaucoma at various stages. While RNFL thickness has remained a key structural parameter to link with visual function, recent studies investigated parameters related to the LC. Ren et al[11] found that a deep LC was associated with worse VF in young glaucomatous eyes; in contrast, Park et al[12] reported that LC depth (LCD) was not correlated with VF loss.

Others have instead investigated dynamic intraocular pressure (IOP)-induced LC changes under the hypothesis that the biomechanical response of the LC to acute changes in IOP could underlie the axonal damage. For instance, Quigley et al[13] reported that glaucomatous eyes with no significant changes in LCD following IOP-lowering procedures had more VF loss than those with significant changes. In a small population with glaucoma, we demonstrated that local LC strains (induced by IOP lowering via trabeculectomy) were associated with VF loss.[14] We believe that deriving such relationships in more patients and in response to acute IOP elevations could be critical for understanding glaucoma pathogenesis and improving glaucoma management.

In this study, we aimed to evaluate the association between glaucomatous functional loss and the biomechanical response of the ONH to acute transient IOP elevations in human eyes in vivo.

Methods

Patient Recruitment

Chinese patients 50 years or older with phakic eyes and no known history of intraocular surgery were recruited from glaucoma clinics at the Singapore National Eye Centre in Singapore. This study was approved by the SingHealth Centralized Institutional Review Board and adhered to the tenets of the Declaration of Helsinki. Written informed consent was obtained from all patients. Primary open-angle glaucoma (POAG) and primary angle-closure glaucoma (PACG) were defined according to the published definitions.[15] Angle closure in an eye was defined as having 2 or more closed quadrants without indentation. All glau-

Key Points

Question Is functional loss in patients with glaucoma associated with the biomechanical response of the optic nerve head to acute transient intraocular pressure elevations?

Findings In this study of 91 patients, functional loss was associated with optic nerve head biomechanics in primary open-angle glaucoma but not in primary angle-closure glaucoma.

Meaning Optic nerve head biomechanics are associated with glaucoma severity in primary open-angle glaucoma, and the 2 primary glaucoma subgroups may exhibit inherently different biomechanical properties.

coma cases had high IOP (>21 mm Hg) at least once after being diagnosed as having glaucomatous optic neuropathy clinically.

Standard Automated Perimetry

Standard automated perimetry (Swedish Interactive Threshold Algorithm standard 24-2 program; Humphrey Field Analyzer II-750i, Carl Zeiss Meditec) was performed at baseline before any procedure was undertaken. A reliable VF examination was defined using the criteria of a false-positive error rate less than 15%[16] and fixation loss less than 33%.[16,17] We did not include false-negative index in our reliability criteria because, although false-negative error is meant to assess participant inattention, failing to respond to stimuli (high false-negative error) may also be a feature of a glaucomatous eye.[18] Indices for VF such as mean deviation (MD) and VF index (VFI) were used in this study. The threshold sensitivities of 52 VF points (in decibels) were clustered and averaged into 6 regions according to Garway-Heath et al[19] to correlate with the corresponding sector of the ONH.
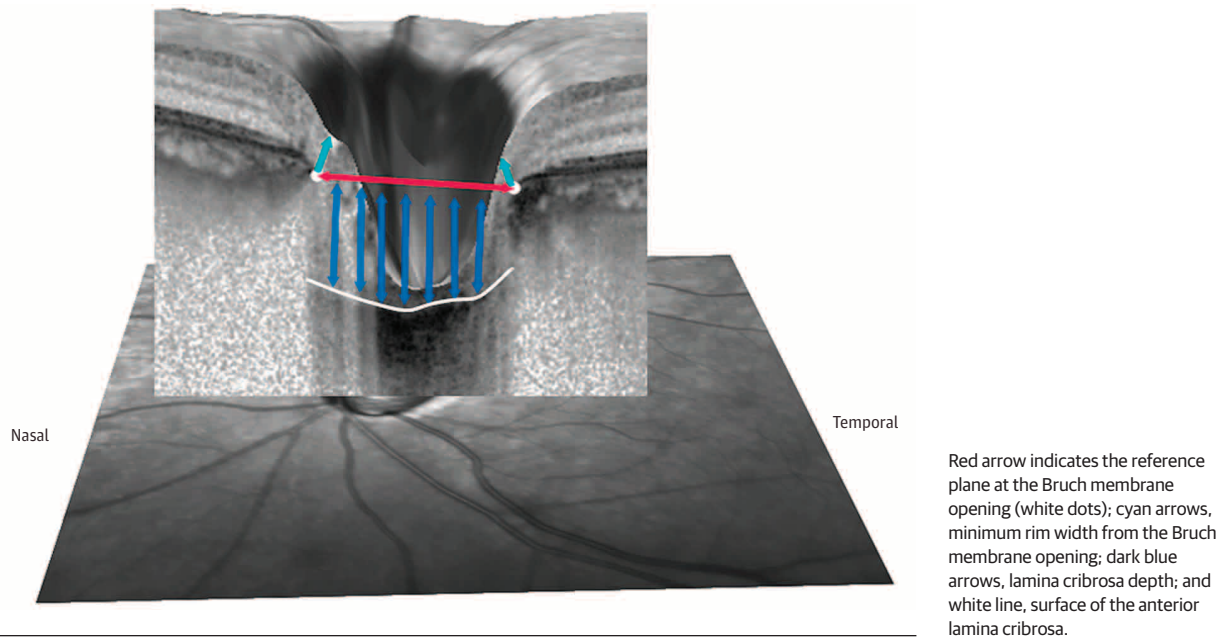
Acute Transient Elevations of IOP

The acute transient IOP elevation model was previously described[20] and validated.[21,22] An ophthalmodynamometer (spring-load indenter) was used to elevate IOP 2 times on 1 eye of each patient. The indenter applied an external force perpendicular to the anterior sclera through the temporal side of the lower eyelid. The applied forces (0.64 N [82.5 g] and then 0.9 N [95 g]) were used to obtain the desired IOP of approximately 35 and 45 mm Hg, respectively. After each IOP increment, IOP was held constant and measured with a Tono-Pen AVIA applanation tonometer (Reichert Inc) while the indenter was maintained in place. The interval between the 2 IOP elevations was 15 minutes. This time was necessary because we believe the first IOP elevation may be responsible for pushing aqueous humor out of the anterior chamber, thus resulting in IOP lowering. After 15 minutes, IOP returned to its approximate baseline value.

OCT and Analysis

The ONH of each patient was imaged 3 times using SD-OCT (Spectralis; Heidelberg Engineering): once before IOP elevation (baseline) and once for each of the 2 IOP elevations. Each OCT volume scan consisted of 97 serial horizontal B-scans

Red arrow indicates the reference plane at the Bruch membrane opening (white dots); cyan arrows, minimum rim width from the Bruch membrane opening; dark blue arrows, lamina cribrosa depth; and white line, surface of the anterior lamina cribrosa.

(30-μm distance between B-scans; 384 A-scans per B-scan; and 20 B-scans averaging) that covered a rectangular area of 15° × 10° centered on the ONH.[21,22] Each imaging session with IOP elevation took approximately 2 to 3 minutes.

Raw SD-OCT images were postprocessed and enhanced using adaptive compensation to remove blood vessel shadows and to improve the visibility of the LC.[23-25] For each eye, the anterior LC and Bruch membrane opening (BMO) of postprocessed OCT volumes were then manually delineated using custom-written MATLAB (MathWorks Inc) algorithms.[21,26] The position of the anterior LC was defined by a sharp increase in axial signal intensity (corresponding to collagen) extending laterally up to the LC insertion points in the peripapillary sclera.[3] The BMO was defined as the end point of the Bruch membrane layer (or retinal pigment epithelium) on either side of the ONH.[27]

Using the aforementioned delineations, we reconstructed the ONH structures in 3-dimensionally and our custom algorithms derived the following parameters according to published protocols.[21,22,26,27]

LC Depth

The LCD was defined as the distance from each anterior LC point to the BMO reference plane. The mean depth of all LC points on the anterior LC surface was reported as the mean LC depth (**Figure 1**).

BMO Area and MRW

The BMO area was defined as the area of the anterior-most boundary of the neural canal. The MRW was defined as the shortest distance from the BMO points to the retinal inner limiting membrane. The MRW measures the thickness of nerve fibers or axons at the NRR (Figure 1).[27] The MRW values were fur-

ther empirically categorized into 6 sectors, comprising four 45° sectors (superior temporal, superior nasal, inferior temporal and inferior nasal) and two 90° sectors (temporal and nasal).

Statistical Analysis

Statistical analyses were performed using SPSS for Windows software version 19.0 (IBM Corp). Continuous variables were described as the mean and standard deviation. We used the Spearman rank correlation coefficient (ρ) to assess the associations between functional loss and ONH structural parameters at baseline, and between functional losses and changes in MRW regionally to acute IOP elevations. The ONH structural changes (Δ) were calculated for each parameter as percentage Changes ([Baseline Value – Value at IOP Elevation/ Baseline Value] ×100). A positive ΔLCD value denotes the anterior LC displacement to acute IOP elevations (toward the vitreous humor), whereas a negative value indicates that the LC was displaced posteriorly. We used linear regression models to assess acute IOP-induced structure-function relationship in each group after adjusting for age, sex, and baseline IOP.

Results

Demographic and Clinical Characteristics

Ninety-one Chinese patients (23 with POAG, 45 with PACG, and 23 without glaucoma; 39 [42.9%] female; mean [SD] age, 65.48 [7.23] years) were included in the final analysis after excluding 10 patients (2 of whom had poor LC visibility due to cataract or uncorrectable blood vessel shadowing and 8 of whom had unreliable VF test results after 2 attempts). **Table 1** shows the demographic and clinical characteristics of the 91 patients. The PACG eyes, as compared

Table 1. Demographic and Clinical Characteristics of the 91 Study Participants

Characteristic	Mean (SD)		
	PACG (n = 45)	POAG (n = 23)	Nonglaucomatous (n = 23)
Age, y	68.36 (6.27)	65 (7.67)	60.35 (5.62)
Female, No. (%)	18 (40.0)	5 (21.7)	16 (69.6)
IOP, mm Hg			
Baseline	16.76 (3.19)	18.35 (3.24)	16.43 (2.21)
First elevation	36.6 (6.40)	36.17 (7.79)	36.43 (6.58)
Second elevation	45.56 (6.34)	46.09 (7.20)	44.83 (7.52)
Spherical equivalent, D	0.03 (2.76)	−1.20 (3.53)	−0.48 (3.18)
Central corneal thickness, μm	534.66 (35.38)	558.42 (32.82)	556.57 (30.95)
Anterior chamber depth, mm	2.94 (0.73)	3.16 (0.38)	3.32 (0.75)
Axial length, mm	23.27 (1.33)	24.56 (1.51)	24.25 (1.29)
Mean deviation of SAP, dB	−5.64 (3.88)	−6.04 (5.48)	−1.96 (1.37)
Visual field index of SAP, %	88.09 (10.76)	85.91 (13.68)	97.52 (1.90)
Baseline anterior LCD, μm[a]	424.4 (123.84)	482.3 (144.56)	391.91 (83.93)
Baseline BMO area, mm²	2.36 (0.53)	2.48 (0.67)	2.13 (0.46)
Baseline MRW, μm[a]	175.20 (54.14)	167.48 (54.04)	296.87 (42.40)

Abbreviations: BMO, Bruch membrane opening; IOP, intraocular pressure; LCD, lamina cribrosa depth; MRW, minimum rim width; PACG, primary angle-closure glaucoma; POAG, primary open angle glaucoma; SAP, standard automated perimetry.

[a] From BMO reference plane.

Table 2. Spearman Rank Correlation Between Functional and Structural Parameters at Baseline

Variable at Baseline	MD of SAP		VFI of SAP	
	ρ (95% CI)	P Value	ρ (95% CI)	P Value
PACG (n = 45)				
Anterior LCD[a]	0.20 (−0.10 to 0.47)	.20	0.16 (−0.14 to 0.43)	.30
BMO area	0.14 (−0.16 to 0.42)	.35	0.07 (−0.23 to 0.36)	.66
MRW[a]	0.30 (0.01 to 0.55)	.06	0.31 (0.02 to 0.55)	.04
Nonglaucomatous controls (n = 23)				
Anterior LCD[a]	−0.19 (−0.56 to 0.24)	.39	−0.60 (−0.81 to −0.25)	.002
BMO area	−0.16 (−0.54 to 0.27)	.46	−0.11 (−0.50 to 0.32)	.61
MRW[a]	0.01 (−0.33 to 0.49)	.98	0.26 (−0.17 to 0.61)	.24
POAG (n = 23)				
Anterior LCD[a]	−0.07 (−0.47 to 0.35)	.74	−0.18 (−0.55 to 0.25)	.42
BMO area	0.27 (0.16 to 0.61)	.21	0.20 (−0.23 to 0.57)	.37
MRW[a]	0.68 (0.37 to 0.85)	<.001	0.70 (0.41 to 0.86)	<.001
All glaucoma cases (n = 68)				
Anterior LCD[a]	0.10 (−0.14 to 0.33)	.43	0.04 (−0.20 to 0.28)	.73
BMO area	0.19 (−0.05 to 0.41)	.11	0.11 (−0.13 to 0.34)	.38
MRW[a]	0.44 (0.23 to 0.61)	<.001	0.46 (0.25 to 0.63)	<.001

Abbreviations: BMO, Bruch membrane opening; LCD, lamina cribrosa depth; MD, mean deviation; MRW, minimum rim width; PACG, primary angle-closure glaucoma; POAG, primary open-angle glaucoma; SAP, standard automated perimetry; VFI, visual field index.

[a] Bruch membrane opening reference plane.

with POAG eyes, had significantly thinner central corneal thickness (mean [SD], 534.66 [35.38] vs 558.42 [32.82] μm; $P = .04$) and smaller axial length (mean [SD], 23.27 [1.33] vs 24.56 [1.51] mm; $P = .02$). Patients with PACG were older than patients without glaucoma (mean [SD] age, 68.36 [6.27] vs 60.35 [5.62] years; $P < .001$), but there was no significant difference in age between patients with PACG and those with POAG (mean [SD] age, 68.36 [6.27] vs 65.00 [7.67] years; $P = .14$).

There was no significant difference in BMO area at baseline, IOP at baseline, and IOP at both elevations among the groups (all $P > .05$). The mean (SD) en face visibility of the anterior LC was relatively good (81.36% [14.25%] of en face BMO area) (Table 1).

Structure-Function Associations at Baseline With POAG and PACG

For all glaucoma cases, a thinner MRW was associated with worse MD ($ρ = 0.44$; 95% CI, 0.23-0.61; $P < .001$) or with worse VFI ($ρ = 0.46$; 95% CI, 0.25-0.63; $P < .001$) at baseline (Table 2). This association held true for each glaucoma group (PACG and POAG). Specifically, a thinner MRW was associated with worse VFI ($ρ = 0.31$; 95% CI, 0.02-0.55; $P = .04$) in PACG eyes and with worse MD ($ρ = 0.68$; 95% CI, 0.37-0.85; $P < .001$) and worse VFI ($ρ = .70$; 95% CI, 0.41-0.86; $P < .001$) in eyes with POAG. The LCD and BMO area at baseline were not associated with MD or VFI in both glaucoma subgroups (all $P > .05$) (Table 2).

Table 3. Linear Regression Model Describing Relationship Between Visual Field and Structural Changes of Optic Nerve Head Following Acute IOP Elevations[a]

% Change	PACG (n = 45)				POAG (n = 23)				Nonglaucomatous (n = 23)			
	MD of SAP		VFI of SAP		MD of SAP		VFI of SAP		MD of SAP		VFI of SAP	
	R (95% CI)	P Value	R (95% CI)	P Value	R (95% CI)	P Value	R (95% CI)	P Value	R (95% CI)	P Value	R (95% CI)	P Value
At first IOP elevation												
ΔLCD[b]	−0.02 (−0.32 to 0.29)	.92	0.03 (−0.27 to 0.32)	.86	−0.64 (−0.97 to −0.31)	.001	−0.57 (−0.94 to −0.19)	.005	0.16 (−0.35 to 0.66)	.53	0.24 (−0.23 to 0.70)	.30
ΔBMO area	0.24 (−0.07 to 0.55)	.12	0.16 (−0.14 to 0.47)	.29	−0.24 (−0.67 to 0.19)	.25	−0.17 (−0.62 to 0.29)	.45	−0.25 (−0.79 to 0.28)	.34	0.17 (−0.35 to 0.68)	.51
ΔMRW[b]	0.07 (−0.28 to 0.41)	.70	−0.03 (−0.36 to 0.31)	.87	−0.48 (−0.86 to −0.09)	.02	−0.57 (−0.94 to −0.2)	.004	0.18 (−0.31 to 0.66)	.46	0.21 (−0.24 to 0.66)	.34
At second IOP elevation												
ΔLCD[b]	−0.05 (−0.36 to 0.27)	.76	−0.01 (−0.32 to 0.29)	.94	−0.26 (−0.70 to 0.19)	.25	−0.25 (−0.71 to 0.20)[c]	.26	0.31 (−0.18 to 0.80)	.20	0.22 (−0.25 to 0.69)	.34
ΔBMO area	0.10 (−0.22 to 0.43)	.53	0.03 (−0.28 to 0.35)	.84	−0.06 (−0.50 to 0.39)	.79	−0.02 (−0.48 to 0.44)[c]	.92	0.09 (−0.47 to 0.65)	.74	−0.26 (−0.77 to 0.25)	.30
ΔMRW[b]	0.08 (−0.24 to 0.39)	.62	0.11 (−0.19 to 0.41)	.47	−0.56 (−0.98 to −0.13)	.01	−0.60 (−10.03 to −0.17)[c]	.008	−0.25 (−0.71 to 0.22)	.28	−0.04 (−0.49 to 0.42)	.86

Abbreviations: BMO, Bruch membrane opening; IOP, intraocular pressure; LCD, lamina cribrosa depth; MD, mean deviation; MRW, minimum rim width; PACG, primary angle-closure glaucoma; POAG, primary open-angle glaucoma; SAP, standard automated perimetry; VFI, visual field index.

[a] After adjusting for age, sex, and baseline IOP. The variables are presented as percentage changes ([baseline − IOP increment]/baseline × 100).

[b] From BMO reference plane.

[c] Values are expressed as β (95% CI).

Associations Between IOP-Induced Structure Changes and Functional Loss

After adjusting for age, sex, and baseline IOP, a greater percentage decrease in MRW in eyes with POAG was associated with worse MD and worse VFI (first IOP elevation, R = −0.48; 95% CI, −0.86 to −0.09; P = .02; and R = −0.57; 95% CI, 0.94 to −0.20; P = .004, respectively; second IOP elevation, R = −0.56; 95% CI, −0.98 to −0.13; P = .01; and R = −0.60; 95% CI, −1.03 to −0.17; P = .008, respectively). However, the percentage decrease in MRW in PACG eyes was not associated with MD or VFI at the first IOP elevation (R = 0.07; 95% CI, −0.28 to 0.41; P = .70; and R = −0.03; 95% CI, −0.36 to 0.31; P = .87, respectively) or at the second IOP elevation (R = 0.08; 95% CI, −0.24 to 0.39; P = .62; and R = 0.11; 95% CI, −0.19 to 0.41; P = .47, respectively) (**Table 3**).

A greater ΔLCD was associated with worse MD (R = −0.64; 95% CI, −0.97 to −0.31; P = .001) (**Figure 2**B) or with worse VFI (R = −0.57; 95% CI, −0.94 to −0.19; P = .005) (Figure 2D) in POAG eyes at the first IOP elevation, after adjusting for age, sex, and IOP at baseline. This result indicated that in POAG eyes the LC with worse VF loss displaced anteriorly in response to acute IOP increase (approximately 35 mm Hg), while the LC with mild VF loss displaced posteriorly. However, this association between ΔLCD and VF indices was not found in PACG eyes at the first IOP elevation (Figure 2A and C). At the second IOP elevation, no such association was found in any of the 2 groups.

The ΔBMO area (akin to change in disc area) at both IOP elevations was not associated with MD or VFI in all groups (all P > .05) (Table 2). There was no significant structure-function association following acute IOP elevations in patients without glaucoma after adjusting for age, sex, and baseline IOP (all P > .05).
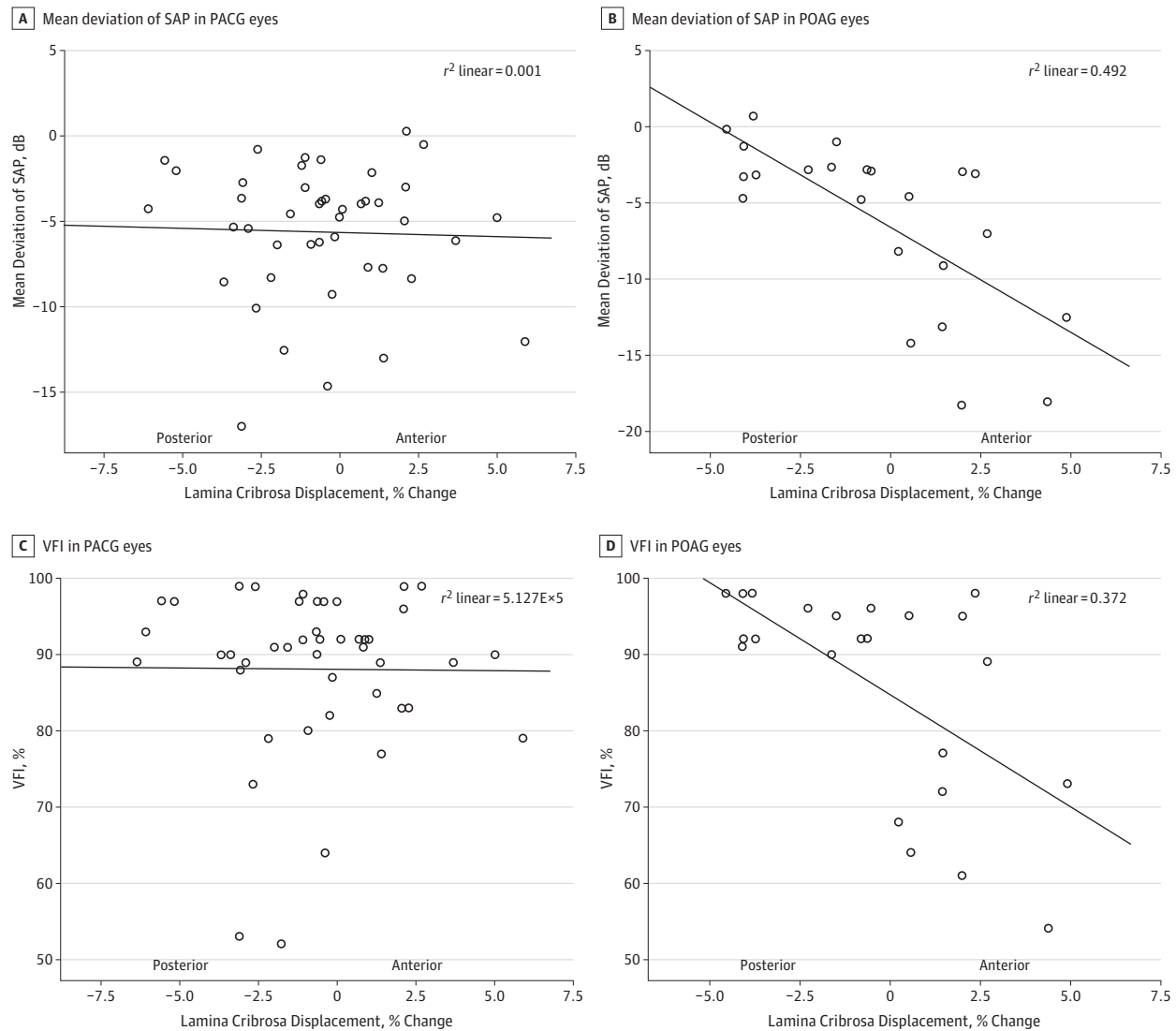
Associations Between IOP-Induced MRW Changes and Threshold Sensitivities Regionally

At the second IOP elevation, an independent association was found between a greater decrease in MRW in the inferior temporal sector and threshold sensitivities of the corresponding VF cluster (ρ = −0.55; 95% CI, −0.78 to −0.18; P = .006) in POAG eyes. No association was found in PACG eyes for any IOP increase (eTable in the Supplement).

Discussion

In this study, we assessed the relationships between established functional loss (detected by standard automated perimetry) and structural changes of the ONH in response to acute transient IOP elevations (derived from OCT). At baseline, we found that a thinner MRW was associated with worse functional loss (assessed by MD or VFI) in both POAG and PACG eyes. Following acute transient IOP elevations, a reduction in MRW was associated with worse functional loss in POAG eyes; however, this relationship was not present in eyes with PACG and eyes without glaucoma. At the first IOP elevation, the LC displaced anteriorly in POAG eyes with worse VF loss but posteriorly when those losses were minimal. Our data suggest that the biomechanical response of the ONH to acute transient IOP

Figure 2. Relationships Between Glaucomatous Visual Field Loss and Lamina Cribrosa Displacement at the First Intraocular Pressure Elevation With Force of 0.64 N

A Mean deviation of SAP in PACG eyes

r^2 linear = 0.001

B Mean deviation of SAP in POAG eyes

r^2 linear = 0.492

C VFI in PACG eyes

r^2 linear = 5.127E×5

D VFI in POAG eyes

r^2 linear = 0.372

The positive data points at the right side of each graph indicate that the lamina cribrosa displaced anteriorly following acute intraocular pressure elevation, whereas the negative values at the left side of each graph indicate that it displaced posteriorly. PACG indicates primary angle-closure glaucoma; POAG, primary open-angle glaucoma; SAP, standard automated perimetry; and VFI, visual field index.

elevations is different between POAG and PACG and may be of importance to improve our understanding of glaucoma pathogenesis.

Baseline MRW and Its Changes With IOP Are Associated With Functional Loss

At baseline, we found that a thinner MRW was associated with worse functional loss, and this relationship was true in both POAG and PACG . These findings might be explained by a loss of ganglion cell axons at onset or during the progression of glaucoma.[1] Other OCT studies have also found an association between MRW and VF indices.[28,29] Our study confirms the association between the severity of glaucoma and MRW (a good surrogate for the number of axons entering the ONH[6]). In ad-

dition, we found that the MRW of glaucomatous eyes were significantly thinner than that of nonglaucomatous eyes at baseline.

An experimental glaucoma study in 51 monkeys showed that MRW thinning exceeded RNFL thinning, suggesting the IOP-related stress and strain could damage the axons not only at the LC but also more dramatically via direct transverse compression within the NRR itself.[30] Thus, it is important to assess the biomechanical response of the NRR (assessed by MRW) together with the LC to get a comprehensive understanding of the 3-dimensional changes associated with IOP elevations. Following acute transient IOP elevations, a greater reduction in MRW in POAG eyes was associated with increased VF loss at both IOP elevations (Table 3) after adjusting for age, sex, and

baseline IOP. However, this relationship was not present in eyes with PACG and or those without glaucoma, suggesting strong biomechanical variabilities across diagnostic groups.

IOP-Induced LCD Changes May Be of Higher Interest Than LCD Alone in Glaucoma Diagnosis and Prognosis

It is important to emphasize that both anterior and posterior displacements of the LC (following changes in IOP) have been observed with SD-OCT by several groups, including ours.[13,14,21,31,32] Following an acute transient IOP elevation, it has been hypothesized that a compliant sclera could yield a larger scleral canal opening, thus pulling the LC taut to displace anteriorly. On the other hand, a stiff sclera could limit scleral canal expansion, thus exposing the LC to the full effects of IOP to make it displace posteriorly.[33,34] However, whether scleral stiffness is solely responsible for LC movements remains to be demonstrated.

We are aware of only 1 study that attempted to link IOP-induced LC movements with VF loss. Quigley et al[13] reported that the LC displacement (either anterior or posterior) was large in eyes with mild VF loss, but minimal or nonexistent in eyes with severe VF loss. This was assessed in 25 POAG eyes and 2 PACG eyes that underwent various IOP-lowering procedures. In contrast, following an acute elevation of IOP, we observed that LCs with more VF loss displaced anteriorly, whereas LCs with less VF loss displaced posteriorly in POAG eyes. Our results suggest that the direction of LC movement (anterior or posterior) following a change in IOP may be an important factor to stratify POAG. However, it is unclear whether this differential behavior would be a result of tissue remodeling in various stages of the disease. This phenomenon (anterior movements with more VF loss) was observed only in POAG eyes but not in PACG eyes, suggesting the possible existence of inherently different mechanisms involved, or similar mechanisms but with different extents of vulnerability of the ONH in the response of IOP-induced stress. Eyes with PACG in this study had shorter axial lengths and might therefore have smaller scleral canals that resist deformations.[35]

An experimental glaucoma study in 9 monkeys found that the ONH's structural changes such as rim area decrement and LC displacement occurred earlier than RNFL thinning.[36] Thus, structural ONH changes (both LC displacement and reduction in MRW) to different IOP levels (achieved with acute IOP models) may provide useful clinical applications to predict the prognosis and progression of glaucoma, particularly for POAG cases. For this study, we recruited only Chinese patients because it is the main ethnicity in Singapore (>70%) and because variations in ONH biomechanical properties could exist across ethnicities.[33] Therefore, our results may not be generalizable to other population groups.

Furthermore, we found that there was no relationship between baseline LCD and VF indices in all cases as well as in PACG and POAG eyes separately. Previous studies have also failed to demonstrate any relationship between the baseline LCD and VF loss.[12,13] Our results suggest that IOP-induced LCD changes may be more useful than LCD alone at any specific time point for prognosis of glaucoma.

Associations Between Regional Changes in MRW and Corresponding VF Clusters

The changes in MRW were assessed not only globally but also sectorially because sectorial variations in MRW have been observed in both nonglaucomatous[27] and glaucomatous[6] eyes. We found that a reduction in MRW in the inferior temporal sector at IOP elevation was independently associated with VF loss in the superior nasal region of the disc in POAG eyes. Pollet-Villard et al[8] reported that the highest correlation was found between baseline MRW in the inferior temporal sector and threshold sensitivity of the corresponding VF sector. We further confirmed this association but from a biomechanical perspective.

Limitations

Several limitations in our work warrant further discussion. First, the IOP elevations may vary among the observers; however, the reported repeatability was good.[21,22] Second, LC visibility was limited in some OCT images and 2 patients were excluded. Third, the BMO reference plane may migrate posteriorly toward the sclera with aging,[37] or when the peripapillary choroid was compressed by acute IOP elevations[32,38]; this may have affected the values of LCD and MRW.[39] Fourth, our OCT sectors' sizes are a slight variation to those ONH sectors defined by Garway-Heath et al.[19] Fifth, our results should hold true if other OCT devices were to be used; however, a proper device comparison analysis should be performed to confirm this. Finally, 9 patients with glaucoma received losartan, and this may have affected their scleral rigidity[40] and thus influenced our results. However, by adding this medication to our statistical models, our results remained the same.

Conclusions

In summary, we established a relationship between functional loss induced by glaucoma and acute IOP-induced structural changes of the ONH. Although the ONH's structural changes induced by acute transient IOP elevations were associated with VF loss in POAG eyes, no association was observed in the PACG group. This suggests a differential biomechanical response (to IOP) in the 2 subgroups of primary glaucoma.

Author Affiliations: Singapore Eye Research Institute and Singapore National Eye Centre, Singapore (Tun, Atalay, Baskaran, Nongpiur, Htoon, Goh, Cheng, Perera, Aung, Strouthidis, Girard); Ophthalmic Engineering and Innovation Laboratory, Department of Biomedical Engineering, National University of Singapore, Singapore (Tun, Girard); Eskisehir Osmangazi University Faculty of Medicine, Eskisehir, Turkey (Atalay); Duke–National University of Singapore Medical School, Singapore

(Baskaran, Htoon, Cheng, Perera, Aung); Department of Ophthalmology, Yong Loo Lin School of Medicine, National University of Singapore, Singapore (Nongpiur, Cheng, Aung); Discipline of Clinical Ophthalmology and Eye Health, University of Sydney, Sydney, Australia (Strouthidis); National Institute for Health Research Biomedical Research Centre, Moorfields Eye Hospital National Health Service Foundation Trust and University College London Institute of Ophthalmology, London, United Kingdom (Strouthidis).

REFERENCES

1. Quigley HA, Addicks EM, Green WR, Maumenee AE. Optic nerve damage in human glaucoma, II: the site of injury and susceptibility to damage. Arch Ophthalmol. 1981;99(4):635-649. .

2. Weinreb RN, Aung T, Medeiros FA. The pathophysiology and treatment of glaucoma: a review. *JAMA*. 2014;311(18):1901-1911.

3. Strouthidis NG, Grimm J, Williams GA, Cull GA, Wilson DJ, Burgoyne CF. A comparison of optic nerve head morphology viewed by spectral domain optical coherence tomography and by serial histology. *Invest Ophthalmol Vis Sci*. 2010;51(3):1464-1474.

4. Sigal IA, Wang B, Strouthidis NG, Akagi T, Girard MJA. Recent advances in OCT imaging of the lamina cribrosa. *Br J Ophthalmol*. 2014;98(suppl 2):34-39. .

5. Chauhan BC, O'Leary N, Almobarak FA, et al. Enhanced detection of open-angle glaucoma with an anatomically accurate optical coherence tomography-derived neuroretinal rim parameter. *Ophthalmology*. 2013;120(3):535-543.

6. Reis ASC, O'Leary N, Yang H, et al. Influence of clinically invisible, but optical coherence tomography detected, optic disc margin anatomy on neuroretinal rim evaluation. *Invest Ophthalmol Vis Sci*. 2012;53(4):1852-1860.

7. Nilforushan N, Nassiri N, Moghimi S, et al. Structure-function relationships between spectral-domain OCT and standard achromatic perimetry. *Invest Ophthalmol Vis Sci*. 2012;53(6):2740-2748.

8. Pollet-Villard F, Chiquet C, Romanet J-P, Noel C, Aptel F. Structure-function relationships with spectral-domain optical coherence tomography retinal nerve fiber layer and optic nerve head measurements. *Invest Ophthalmol Vis Sci*. 2014;55(5):2953-2962.

9. Leite MT, Zangwill LM, Weinreb RN, Rao HL, Alencar LM, Medeiros FA. Structure-function relationships using the cirrus spectral domain optical coherence tomograph and standard automated perimetry. *J Glaucoma*. 2012;21(1):49-54.

10. Muth DR, Hirneiß CW. Structure-function relationship between Bruch's membrane opening-based optic nerve head parameters and visual field defects in glaucoma. *Invest Ophthalmol Vis Sci*. 2015;56(5):3320-3328.

11. Ren R, Yang H, Gardiner SK, et al. Anterior lamina cribrosa surface depth, age, and visual field sensitivity in the Portland Progression Project. *Invest Ophthalmol Vis Sci*. 2014;55(3):1531-1539.

12. Park SC, Brumm J, Furlanetto RL, et al. Lamina cribrosa depth in different stages of glaucoma. *Invest Ophthalmol Vis Sci*. 2015;56(3):2059-2064.

13. Quigley H, Arora K, Idrees S, et al. Biomechanical responses of lamina cribrosa to intraocular pressure change assessed by optical coherence tomography in glaucoma eyes. *Invest Ophthalmol Vis Sci*. 2017;58(5):2566-2577.

14. Girard MJA, Beotra MR, Chin KS, et al. In vivo 3-dimensional strain mapping of the optic nerve head following intraocular pressure lowering by trabeculectomy. *Ophthalmology*. 2016;123(6):1190-1200.

15. Foster PJ, Buhrmann R, Quigley HA, Johnson GJ. The definition and classification of glaucoma in prevalence surveys. *Br J Ophthalmol*. 2002;86(2):238-242.

16. Atalay E, Nongpiur ME, Yap SC, et al. Pattern of visual field loss in primary angle-closure glaucoma across different severity levels. *Ophthalmology*. 2016;123(9):1957-1964.

17. Keltner JL, Johnson CA, Cello KE, et al; Ocular Hypertension Treatment Study Group. Classification of visual field abnormalities in the ocular hypertension treatment study. *Arch Ophthalmol*. 2003;121(5):643-650.

18. Heijl A, Patella VM, Bengtsson B. The Field Analyzer Primer: Effective Perimetry. 4th ed. Dublin, CA: Carl Zeiss Meditec; 2012. https://www.academia.edu/2183305/Effective_Perimetry_Zeiss_Visual_Field_Primer_4th_Edition_._Heijl_Bengtsson_and_Patella_2012_. Accessed March 6, 2017.

19. Garway-Heath DF, Poinoosawmy D, Fitzke FW, Hitchings RA. Mapping the visual field to the optic disc in normal tension glaucoma eyes. *Ophthalmology*. 2000;107(10):1809-1815.

20. Agoumi Y, Sharpe GP, Hutchison DM, Nicolela MT, Artes PH, Chauhan BC. Laminar and prelaminar tissue displacement during intraocular pressure elevation in glaucoma patients and healthy controls. *Ophthalmology*. 2011;118(1):52-59.

21. Tun TA, Thakku SG, Png O, et al. Shape changes of the anterior lamina cribrosa in normal, ocular hypertensive, and glaucomatous eyes following acute intraocular pressure elevation. *Invest Ophthalmol Vis Sci*. 2016;57(11):4869-4877.

22. Sharma S, Tun TA, Baskaran M, et al Effect of acute intraocular pressure elevation on the minimum rim width in normal, ocular hypertensive and glaucoma eyes [published online May 10, 2017]. *Br J Ophthalmol*. doi:10.1136/bjophthalmol-2017-310232

23. Girard MJA, Strouthidis NG, Ethier CR, Mari JM. Shadow removal and contrast enhancement in optical coherence tomography images of the human optic nerve head. *Invest Ophthalmol Vis Sci*. 2011;52(10):7738-7748.

24. Mari JM, Strouthidis NG, Park SC, Girard MJ. Enhancement of lamina cribrosa visibility in optical coherence tomography images using adaptive compensation. *Invest Ophthalmol Vis Sci*. 2013;54(3):2238-2247.

25. Girard MJ, Tun TA, Husain R, et al. Lamina cribrosa visibility using optical coherence tomography: comparison of devices and effects of image enhancement techniques. *Invest Ophthalmol Vis Sci*. 2015;56(2):865-874.

26. Thakku SG, Tham YC, Baskaran M, et al. A global shape index to characterize anterior lamina cribrosa morphology and its determinants in healthy Indian eyes. *Invest Ophthalmol Vis Sci*. 2015;56(6):3604-3614.

27. Tun TA, Sun CH, Baskaran M, et al. Determinants of optical coherence tomography-derived minimum neuroretinal rim width in a normal Chinese population. *Invest Ophthalmol Vis Sci*. 2015;56(5):3337-3344.

28. Danthurebandara VM, Sharpe GP, Hutchison DM, et al. Enhanced structure-function relationship in glaucoma with an anatomically and geometrically accurate neuroretinal rim measurement. *Invest Ophthalmol Vis Sci*. 2014;56(1):98-105.

29. Mizumoto K, Gosho M, Zako M. Correlation between optic nerve head structural parameters and glaucomatous visual field indices. *Clin Ophthalmol*. 2014;8:1203-1208.

30. Fortune B, Reynaud J, Hardin C, Wang L, Sigal IA, Burgoyne CF. Experimental glaucoma causes optic nerve head neural rim tissue compression: a potentially important mechanism of axon injury. *Invest Ophthalmol Vis Sci*. 2016;57(10):4403-4411.

31. Wu Z, Lin C, Crowther M, Mak H, Yu M, Leung CK-S. Impact of rates of change of lamina cribrosa and optic nerve head surface depths on visual field

progression in glaucoma. *Invest Ophthalmol Vis Sci.* 2017;58(3):1825-1833.

32. Fazio MA, Johnstone JK, Smith B, Wang L, Girkin CA. Displacement of the lamina cribrosa in response to acute intraocular pressure elevation in normal individuals of African and European descent. *Invest Ophthalmol Vis Sci.* 2016;57(7): 3331-3339.

33. Sigal IA, Yang H, Roberts MD, Burgoyne CF, Downs JC. IOP-induced lamina cribrosa displacement and scleral canal expansion: an analysis of factor interactions using parameterized eye-specific models. *Invest Ophthalmol Vis Sci.* 2011;52(3):1896-1907.

34. Sigal IA, Ethier CR. Biomechanics of the optic nerve head. *Exp Eye Res.* 2009;88(4):799-807.

35. Bellezza AJ, Hart RT, Burgoyne CF. The optic nerve head as a biomechanical structure: initial finite element modeling. *Invest Ophthalmol Vis Sci.* 2000;41(10):2991-3000.

36. Strouthidis NG, Fortune B, Yang H, Sigal IA, Burgoyne CF. Longitudinal change detected by spectral domain optical coherence tomography in the optic nerve head and peripapillary retina in experimental glaucoma. *Invest Ophthalmol Vis Sci.* 2011;52(3):1206-1219.

37. Johnstone J, Fazio M, Rojananuangnit K, et al. Variation of the axial location of Bruch's membrane opening with age, choroidal thickness, and race. *Invest Ophthalmol Vis Sci.* 2014;55(3):2004-2009.

38. Strouthidis NG, Fortune B, Yang H, Sigal IA, Burgoyne CF. Effect of acute intraocular pressure elevation on the monkey optic nerve head as detected by spectral domain optical coherence tomography. *Invest Ophthalmol Vis Sci.* 2011;52(13): 9431-9437.

39. Vianna JR, Lanoe VR, Quach J, et al. Serial changes in lamina cribrosa depth and neuroretinal parameters in glaucoma: impact of choroidal thickness. *Ophthalmology.* 2017;124(9):1392-1402.

40. Quigley HA, Cone FE. Development of diagnostic and treatment strategies for glaucoma through understanding and modification of scleral and lamina cribrosa connective tissue. *Cell Tissue Res.* 2013;353(2):231-244.